Circulation Journal
Circ J 2020; 84: 235–244
doi:10.1253/circj.CJ-19-0926

ORIGINAL ARTICLE
Pediatric Cardiology and Adult Congenital Heart Disease

Simultaneous Volumetric and Functional Assessment of the Right Ventricle in Hypoplastic Left Heart Syndrome After Fontan Palliation, Utilizing 3-Dimensional Speckle-Tracking Echocardiography

Tomoyuki Sato, MD, PhD; Renzo JC Calderon, MD; Berthold Klas, BSc; Gianni Pedrizzetti, PhD; Anirban Banerjee, MD

Background: Right ventricular (RV) volumetric and functional assessments are both crucial for the management of patients with hypoplastic left heart syndrome (HLHS). 3-dimensional echocardiography (3DE) for volume measurements and 2D speckle-tracking echocardiography (2D-STE) for strain analysis are performed separately. 3D-STE is capable of evaluating those parameters simultaneously and providing principal strain (PS), unifying the concepts of myofiber orientation and contraction into a single, maximal contractile direction. However, the application of 3D-STE to HLHS has not been studied and so became the aim of our study.

Methods and Results: 64 HLHS patients after Fontan palliation underwent 3D-STE analysis measuring RV end-diastolic volume index (EDVi), ejection fraction (EF), global PS (GPS), global circumferential strain (GCS), and global longitudinal strain (GLS). Volume measurements were compared between 3D-STE and 3DE, and strains were compared between 3D- and 2D-STE. EDVi and EF showed strong correlations between 3D-STE and 3DE (r=0.93 and 0.87, respectively). GCS and GLS showed moderate correlations between 3D- and 2D-STE (r=0.65 and 0.61, respectively). GPS showed highest magnitude and excellent correlation with EF (r=−0.95).

Conclusions: Simultaneous volumetric and functional assessment by 3D-STE was a useful method in this HLHS cohort. PS is a promising parameter for evaluating the RV function of HLHS, which could be useful during longitudinal follow-up.

Key Words: 3-dimensional speckle-tracking echocardiography; Hypoplastic left heart syndrome; Principal strain

Right ventricular (RV) dysfunction poses an important problem in patients with hypoplastic left heart syndrome (HLHS) compared with other morphologic types of single ventricles.[1,2] Systolic dysfunction and ventricular dilation after Fontan palliation are future risk factors that lead to increased mortality and heart transplants in the HLHS cohort.[3] Therefore, quantitative and repeatable assessment of RV volume and function would be advantageous in the longitudinal management of HLHS patients after Fontan palliation. Quantification of RV function and volume of HLHS by 2-dimensional echocardiography has remained a challenge and these parameters are often assessed qualitatively (eye-ball method) in everyday practice.[4] Consequently, the quantitative measurements of volume and function by cardiac magnetic resonance imaging (CMRI) are currently considered as the gold standard,[5] although it is not suitable for frequent assessments during regular outpatient evaluations.

On the other hand, 3D echocardiography (3DE) has been shown to be a possible alternative for measuring RV volume in HLHS.[6–9] Additionally, 2D speckle-tracking echocardiography (STE) has been recognized as a useful method for assessing not only ventricular function but also the mechanics of ventricular function in HLHS.[10,11] More recently, the advent of 3D-STE has allowed us to measure the 3D ventricular volumes and strains simultaneously in the left ventricle (LV).[12]

Current functional analyses by 2D strain provide predominantly axis-dependent measurement of ventricular deformation, such as longitudinal strain (LS), circumferential strain (CS) and radial strain (RS). This approach does not accommodate the 3D nature of the myocardium, where the multidirectional sliding motion of tissue planes, known as "shear", occurs throughout the cardiac cycle. Therefore, in a 3D model there are 9 strains: 3 normal and 6 shear. Because shear strains are difficult to measure, a

Received October 22, 2019; revised manuscript received November 22, 2019; accepted December 2, 2019; J-STAGE Advance Publication released online January 11, 2020 Time for primary review: 21 days

Department of Pediatrics, Division of Cardiology, The Children's Hospital of Philadelphia, Philadelphia, PA (T.S., R.J.C.C., A.B.), USA; TomTec Imaging Systems, Munich (B.K.), Germany; and Department of Engineering and Architecture, University of Trieste, Trieste (G.P.), Italy

Mailing address: Tomoyuki Sato, MD, PhD, Department of Pediatrics, Jichi Children's Medical Center Tochigi, 3311-1 Yakushiji, Shimotsuke 329-0498, Japan. E-mail: tomo-st@jichi.ac.jp

ISSN-1346-9843

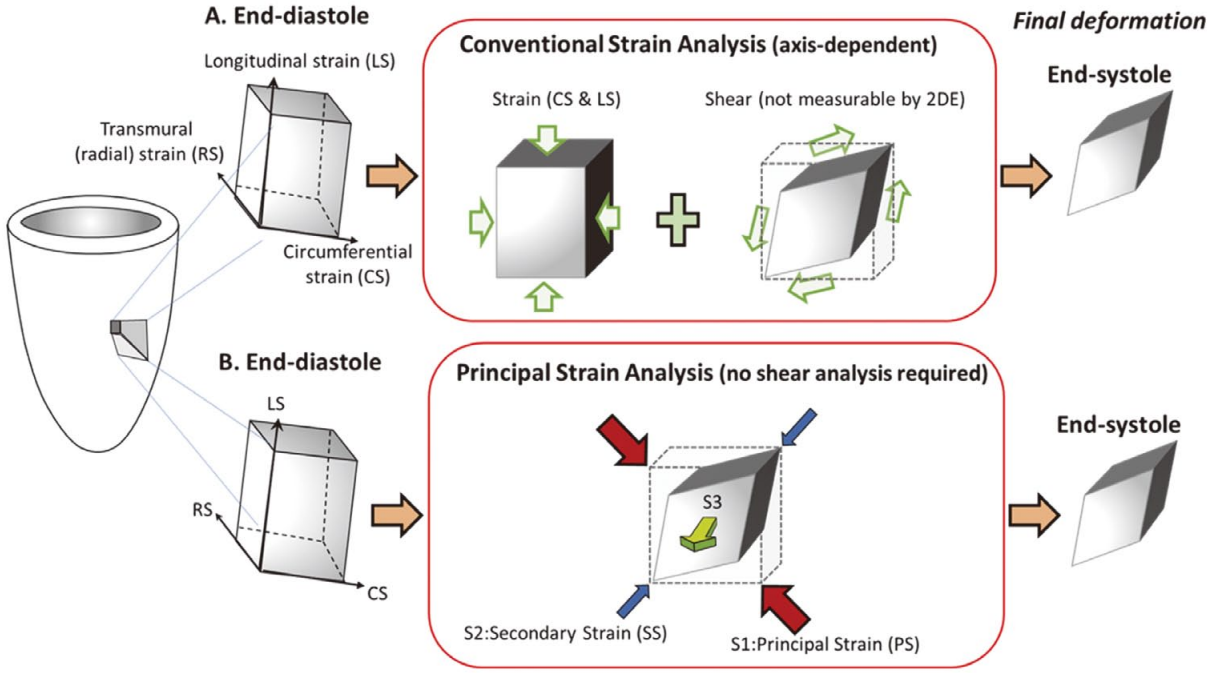

Figure 1. Process of myocardial tissue deformation, showing the 3 orthogonal deformations that completely depict the deformation of a 3D myocardial segment, without the need to consider shear components or the need to limit measurements to conventional axis-dependent directions (longitudinal, circumferential and radial). S1 indicates the PS and is the main contractile force; S2 is the SS, which is transversal to the PS and of much lower intensity; S3 is the positive strain resulting from tissue incompressibility and is mostly represented by thickening of myocardium along the radial direction. The latter cannot be measured by 3D-STE because of the lack of epicardial imaging, but can be measured by cardiac MRI. Moreover, because of tissue incompressibility, S3 is completely dependent on S1 and S2. Therefore, S3 can be excluded and S1 and S2 can provide a simplified, 2-component model of myocardial deformation that is more comprehensive than conventional, axis-dependent strains. 3D, three-dimensional; CS, circumferential strain; LS, longitudinal strain; PS, principal strain; RS, radial strain; SS, secondary strain.

novel method to overcome this limitation is known as principal strain (PS), which is a 3D concept that has been applied extensively in engineering for studying fiber-reinforced materials. However, it is an entirely new concept in the field of cardiology and was introduced only after the advent of 3D-STE. The deformation of a 3D myocardial segment occurs in 3 mutually perpendicular directions, known as eigenvectors: S1, S2, and S3 (**Figure 1**, **Lower panel**). The net effect of these vectors is S1+S2+S3≈0.[13] PS simplifies the concept of 3D deformation, because the shear strains are zero in the orientation of the principal strains. PS defines the direction along the main contractile strain (S1), which is accompanied by a secondary strain (S2) that is typically of much lower intensity and also by a thickening along the radial direction (positive strain, S3, that is a consequence of tissue incompressibility). This approach gives a mechanics-based unification of the 3D deformation pattern from 9 strains into 1 principal strain (S1) (red arrows, **Figure 1**) and 1 secondary strain (S2) (blue arrows, **Figure 1**). The third strain (S3) resulting from tissue incompressibility, is not measurable by 3D echocardiography, because it needs contouring of both endocardium and epicardium. The latter cannot be measured by 3D-STE, because of the lack of epicardial imaging, but can be measured by cardiac MRI.[14] Moreover, because of tissue incompressibility, S3 is completely dependent on S1 and S2. Therefore, S3 can be excluded and S1 and S2 can provide a simplified, 2-component, unidirectional model of myocardial deformation that is more comprehensive than conventional, axis-dependent strains.

However, this method has not been evaluated for the assessment of the RV function in HLHS. 3D-STE, involving PS analysis, may be capable of providing novel insights into the mechanisms of RV function in HLHS maintaining systemic circulation, in addition to the simultaneous volumetric and functional assessments.

The aim of this study had 2 arms, a volumetric arm and a functional arm: (1) evaluate the feasibility of RV volume assessment in HLHS using 3D-STE and (2) evaluate the feasibility of assessing RV function in HLHS from normal and principal strains derived from 3D-STE. We hypothesized that 3D-STE would be a reliable volumetric and functional tool for evaluating RV function in HLHS in everyday practice.

Methods

Subject Population

We analyzed 64 patients with HLHS after Fontan palliation who underwent clinically indicated echocardiography at the outpatient clinic of the Cardiac Center of Children's Hospital of Philadelphia. In order to maintain homogeneity in the cohort, variants of HLHS (i.e., unbalanced atrioventricular canal, double outlet right ventricle, SRV with VSD

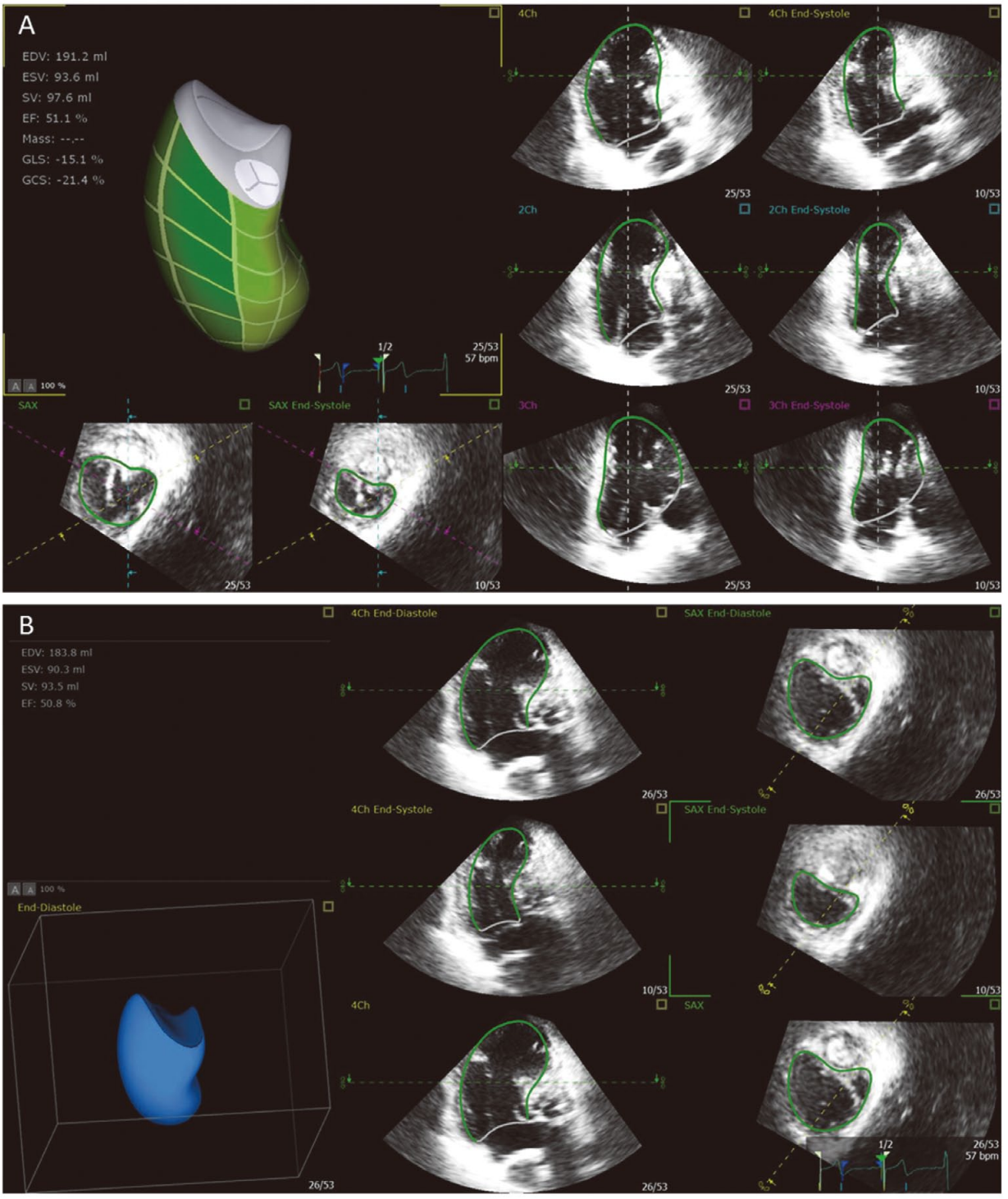

Figure 2. Analysis of 3D-STE and 3DE. (**A**) The right panel shows the 3 apical chamber views (4-, 3-, and 2-chamber) with static and moving images. The lower left panel shows static and moving short-axis images. The 3D image is reconstructed in the top left panel. The endocardial border is automatically tracked throughout the cardiac cycle in 3D-STE (see **Supplementary Movie 1**) (**B**) The right panel shows static short-axis images at ED and ES and a moving short-axis image. The middle panel shows static apical chamber views at ED and ES and a moving image. The 3D image is reconstructed in the lower left panel. The endocardial border is manually traced only at ED and ES in 3DE (see **Supplementary Movie 2**). 3DE, 3D echocardiography; ED, end-diastole; ES, end-systole; STE, speckle-tracking echocardiography; other abbreviations as in Figure 1.

Table 1. Demographic Characteristics of HLHS Cohort

Variable	Value
Age (years)	10.6 (2.4–18.4)
Female	28 (43.8)
Duration after Fontan (years)	7.3 (0.1–16.4)
Weight (kg)	28.1 (11.2–76.1)
Oxygen saturation (%)	92 (76–99)
Heart rate (beats/min)	76 (44–124)
Systolic BP (mmHg)	106 (75–148)
Diastolic BP (mmHg)	59 (38–79)
Anatomy	
MA/AA	29 (45.3)
MS/AA	16 (25.0)
MS/AS	19 (29.7)
Type of stage 1 palliation	
Blalock-Taussig shunt	44 (68.7)
Sano shunt	20 (31.3)
Type of Fontan	
LT	26 (40.6)
EC	38 (59.4)
Fenestration	46 (71.9)
Complications	
TR ≥moderate	10 (15.6)
PLE	6 (9.4)
Plastic bronchitis	3 (4.7)
Pacemaker implantation	3 (4.7)
Other (TVR, stroke)	2 (3.1)

Data expressed as median (range) or number (%). AA, aortic atresia; AS, aortic stenosis; BP, blood pressure; EC, extra-cardiac conduit; LT, lateral tunnel; MA, mitral atresia; MS, mitral stenosis; PLE, protein-losing enteropathy; TR, tricuspid regurgitation; TVR, tricuspid valve replacement.

and critical aortic stenosis with endocardial fibroelastosis in the LV) were excluded. The study was approved by the Institutional Review Board of The Children's Hospital of Philadelphia and all participants provided informed consent before we obtained the research images.

3D Echocardiography

3DE was performed by experienced cardiac sonographers using the iE33 ultrasound system (Philips Medical Systems, Andover, MA, USA) with X3-1 or X5-1 matrix array transducers optimizing the patient's size. 3D full-volume datasets were acquired from the apical transducer position, taking care to cover the entire RV, including its apex, during breath holding or quiet breathing. The 3D datasets consisted of 4 or 6 subvolumes with ECG gating at the highest possible frame rate (median 32, range 18–34 frames/s). We obtained several 3D datasets for each patient, and selected the best image without stitch artifacts. The 3D datasets were exported to a research workstation at the native frame rate.

Volume Measurement and Strain Analysis by 3D-STE

3D-STE was analyzed using commercially used software (4D LV-Analysis version 3.1; TomTec Imaging Systems, Munich, Germany) applied to the RV of HLHS patients as follows: (1) brightness and contrast adjusted to enhance the RV endocardial borders; (2) the RV long-axis manually aligned from the center of the tricuspid valve to the RV apex in the 3 apical views (4-, 3-, and 2-chamber views) and the reference point of the aortic valve was placed at the neo-aortic valve (native pulmonary valve); (3) the endocardial surface was identified by the software, and then manually adjusted along the endocardial border, defined as the border along the recesses of the RV trabeculations; (4) the software automatically tracked the border throughout the cardiac cycle (**Figure 2A**, **Supplementary Movie 1**) and when necessary, manual correction was applied to the automatically detected endocardial borders; and (5) the software computed the end-diastolic volume (EDV), end-systolic volume (ESV), ejection fraction (EF), and various strains (PS, CS, and LS).

Volume Measurement by 3DE

For comparison, we measured the RV volumes in the HLHS patients using another commercially used 3DE software (4D Cardio-View version 3; TomTec Imaging Systems), which has a more established 3D technique and is very similar in function to the software used in previous studies.[6,7] It requires manual selections of the ED and ES frames visually defined as the largest and smallest chamber dimensions. The analysis was performed as follows: (1) the RV long-axis was aligned and the reference aortic valve was placed in a manner similar to that in the 3D-STE analysis; (2) the frame at ED was selected as the visually largest ventricular size and/or the frame at the time the tricuspid valve closure and the frame at ES was selected as the visually smallest ventricular size and/or the frame just before the tricuspid valve opening; (3) using still and motion frames, the endocardial borders were manually traced at ED and ES in the apical and short-axis views; and (4) based on these tracings, the EDV, ESV, and EF were calculated (**Figure 2B**, **Supplementary Movie 2**).

Strain Analysis by 2D-STE

The 2D RV apical 4-chamber and basal short-axis images were acquired at the median frame rate of 61 (range 50–79) frames/s and exported to a research workstation at the native frame rate. 2D-STE was analyzed by 2D cardiac performance analysis (2D CPA 1.3.0.91, TomTec Imaging Systems) in 3 steps: (1) single-beat cine loop including the entire RV chamber was selected; (2) the RV endocardial border was manually traced at ES; and (3) the software automatically performed the endocardial border tracking and computed LS from 4-chamber images and CS from basal short-axis images.

Statistical Analysis

All continuous data were assessed for normality using the Shapiro-Wilk test and expressed as mean ± standard deviation (SD) or median (range), unless otherwise stated. Differences in the measurements between different techniques were assessed by Student's t-test or Mann-Whitney U test depending on the data distribution. RV volumes from 3D-STE were compared with those from 3DE using linear regression with Spearman's correlation coefficients, and global CS (GCS) and global LS (GLS) from 3D-STE were compared with those from 2D-STE using linear regression with Pearson's correlation coefficients. Global PS (GPS), GCS, and GLS were compared by one-way ANOVA with post hoc analysis. Correlations between EF and 3D strains were calculated by Spearman's correlation coefficients, and then significances of difference between correlations were assessed. We accepted $P<0.05$ or when

Table 2. Overall Values Derived From 3D-STE, 3DE, and 2D-STE

Variable	3D-STE (n=64)	3DE (n=64)	2D-STE (n=58)
EDVi (mL/m²)	94.5 (57.6–183.5)	92.8 (54.5–164.2)	
ESVi (mL/m²)	45.7 (23.2–141.5)	47.4 (28.5–126.6)	
EF (%)	51.2 (22.9–64.2)	47.7 (22.9–59.5)	
GPS (%)	−28.4±4.7*		
GCS (%)	−22.9±4.7†		−17.8±4.2
GLS (%)	−18.2±3.3		−18.7±3.8

Data expressed as median (range) in volume measurements and mean±SD in strains. *P<0.01 vs. GCS and GLS in 3D-STE, †P<0.01 vs. GLS in 3D-STE. 2D, 2-dimensional; 3D, 3-dimensional; 3DE, 3D echocardiography; EDVi, end-diastolic volume index; EF, ejection fraction; ESVi, end-systolic volume index; GCS, global circumferential strain; GLS, global longitudinal strain; GPS, global principal strain; STE, speckle-tracking echocardiography.

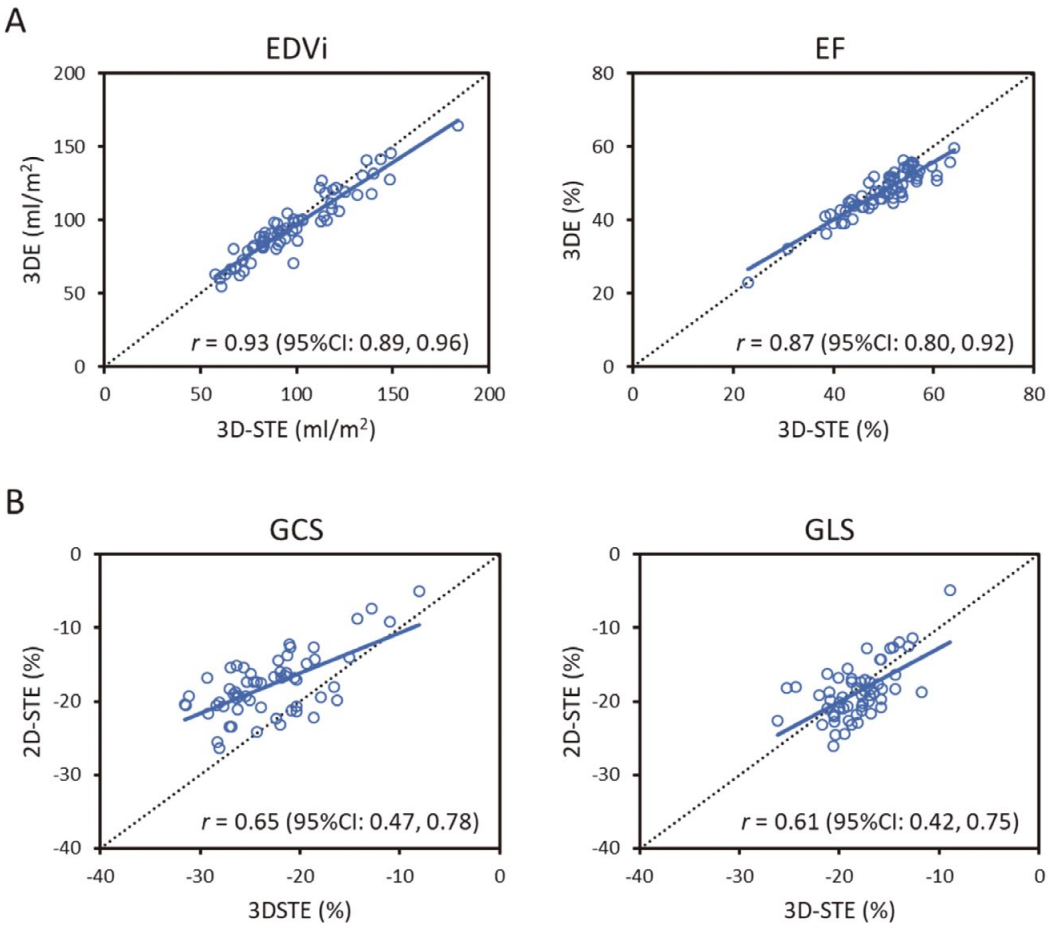

Figure 3. Linear regressions between different methods (3D-STE vs. 3DE and 3D-STE vs. 2D-STE). Dashed and solid lines indicate absolute agreement and estimated linear regression, respectively. (**A**) Regression models between 3D-STE and 3DE are shown in EDVi (**Left**) and EF (**Right**). They indicate strong correlations. (**B**) Regression models between 3D-STE and 2D-STE are shown in GCS (**Left**) and GLS (**Right**). They indicate moderate correlations. 2D, two-dimensional; EDVi, end-diastolic volume index; EF, ejection fraction; GCS, global circumferential strain; GLS, global longitudinal strain; other abbreviations as in Figures 1 and 2.

the 95% confidence interval did not include 0 as indicating statistical significance. All statistical analyses were performed with EZR (Version 1.37; Saitama Medical Center, Jichi Medical University, Saitama, Japan), which is a graphical user interface for R (version 3.4.1; The R Foundation for Statistical Computing, Vienna, Austria).

Reproducibility

For interobserver variability, 25 patients were selected randomly and the analysis was repeated de novo by a

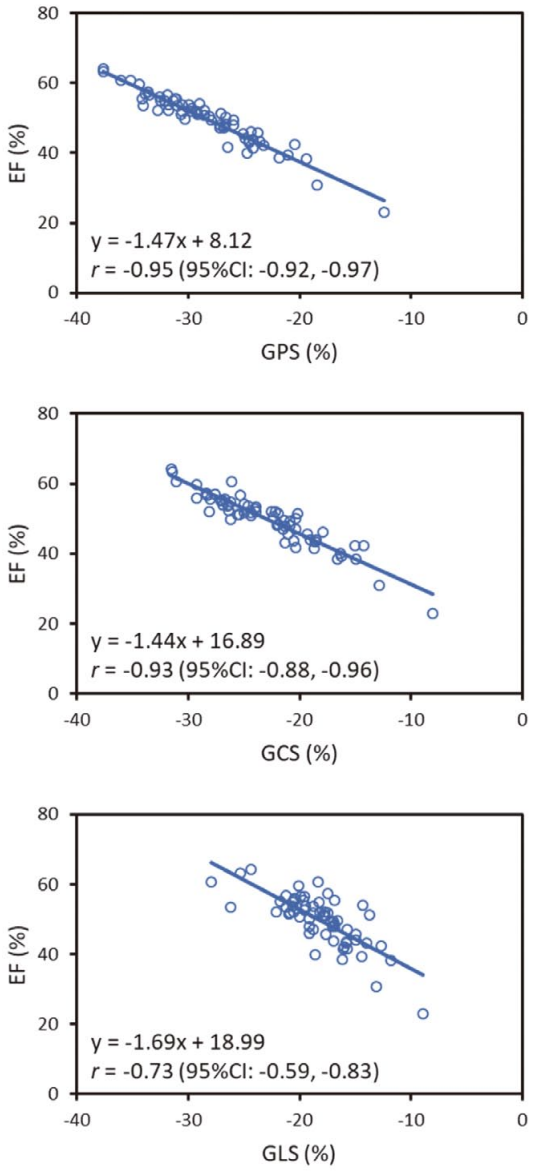

Figure 4. Linear regressions showing the correlations between strains and EF in 3D-STE analysis. All strains show strong correlations with EF, however, correlation coefficients of GPS (**Upper**) and GCS (**Middle**) show significantly higher than GLS (**Lower**). GPS, global principal strain; other abbreviations as in Figures 1–3.

second blinded investigator. For intra-observer variability, one observer repeated the measurements after 4 weeks. Intra- and interobserver variability was evaluated by intra-class correlation coefficients (ICCs) and Bland-Altman plots of percentage difference.

Results

The patient demographics, including anatomy of HLHS, type of stage 1 palliation, type of Fontan, and complications, are shown in **Table 1**. Overall results from 3D-STE, 3DE, and 2D-STE are displayed in **Table 2**. In the 2D-STE analysis, 6 of 64 patients were excluded because of insufficient quality of 2D images.

Comparison of Volume Measurements: 3D-STE vs. 3DE

We compared volume measurements in all 64 patients. **Figure 3A** shows the strong correlations in EDV indexed by body surface area (EDVi) and EF (r=0.93 and 0.87, respectively).

Comparison of Strain Analysis: 3D-STE vs. 2D-STE

We compared the 3D- and 2D-strain values in 58 patients. The magnitude of 3D-GCS was higher than that of 2D-GCS (−23.0±5.0 vs. −17.8±4.2, respectively), while the magnitude of 3D-GLS was not significantly different from that of 2D-GLS (−18.1±3.1 vs. −18.7±3.8, respectively). **Figure 3B** shows the moderate correlations in GCS and GLS (r=0.65 and 0.61, respectively).

Contribution of Strains to RV Function in HLHS

We assessed the contribution of strains to RV function in all 64 patients with HLHS. GPS revealed the highest magnitude compared with GCS and GLS in the 3D-STE analysis (**Table 2**). GPS had the strongest correlation with EF among all strains, although it was not significantly different compared with GCS (**Figure 4**).

Intra- and Interobserver Variability

Intra- and interobserver variability was assessed in 25 randomly selected patients. ICCs of intra-observer variability were 0.95, 0.95, and 0.86 in EDVi, EF, and GPS, respectively, and those for interobserver variability were 0.94, 0.87, and 0.81, respectively. Bland-Altman plots of percent difference in intra- and interobserver variability are shown in **Figure 5**, which demonstrated good agreement.

Discussion

This study used 3D-STE to describe RV function in HLHS patients after Fontan palliation. The results are 2 valuable pieces of information. First, 3D-STE is a useful method capable of simultaneously evaluating ventricular volume and myocardial deformation of HLHS. Second, PS showed the highest magnitude of strain and correlated strongly with 3D-EF, thereby providing us with a more comprehensive method of describing RV function in HLHS.

RV Volume Measurement in HLHS

Our study demonstrated that 3D-STE was useful for evaluating RV volume in HLHS patients after Fontan palliation. Although quantitative assessment of RV function in HLHS by echocardiography is challenging, 3DE assessment of volumes and EF has been verified as a comparable method with CMRI even in HLHS patients and used in a multicenter clinical study.[7] In our study, we compared the RV volumes obtained with3D-STE with those from 3DE in HLHS patients after Fontan palliation, showing excellent correlations between them. From these results, we suggest that 3D-STE is as useful as 3DE for volume measurement in HLHS patients after Fontan palliation. However, their different methodologies may affect the results. 3D-STE tracks the endocardial border throughout the cardiac cycle, and then the ED and ES frames are defined automatically by the software. In contrast, ED and ES frames are defined manually by the investigator in 3DE, and then the contours of endocardial border are drawn by the investigator for the volume measurements. Therefore, volume measurements

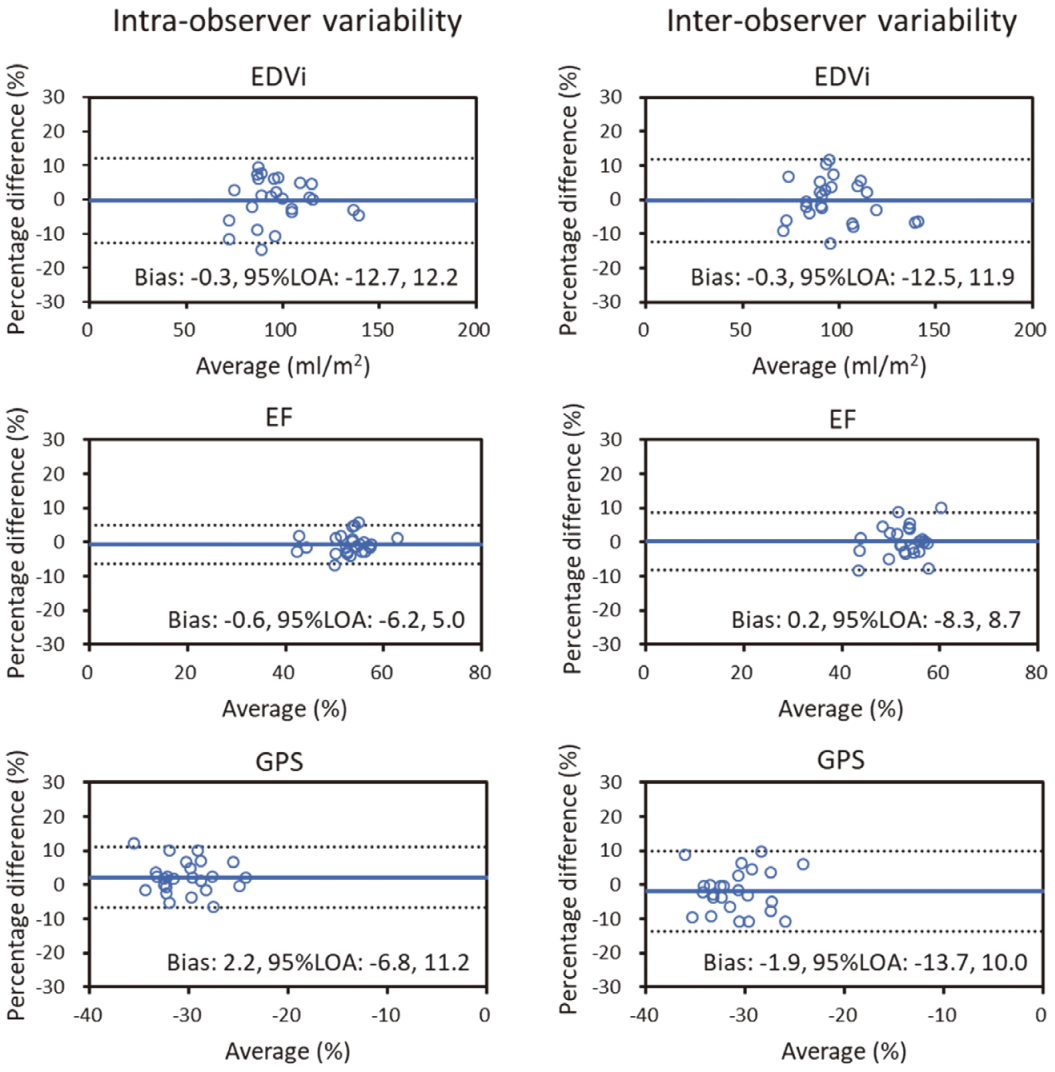

Figure 5. Bland-Altman plots of percent difference in intra- and interobserver variability of 3D-STE. Bias and 95% LOA are expressed as the solid line and dashed lines, respectively. All parameters show good agreements, indicating good reproducibility of 3D-STE. LOA, limits of agreement; other abbreviations as in Figures 1–4.

from 3D-STE may be more accurate and have higher reproducibility than those from 3DE because of less human error in 3D-STE. Moreover, 3D-STE can track the speckles of endocardial border simultaneously for strain analysis, whereas 3DE does not provide any strain measurements. Soriano et al demonstrated that EDV and EF derived from 3DE were significantly smaller than those from CMRI.[6] In addition, Kleijn et al showed that EDV from 3D-STE was also underestimated compared with that from CMRI in the LV.[15] Therefore, RV volume measurements from 3D-STE may also be underestimated compared with those from CMRI even in HLHS, although we did not perform a direct comparison between 3D-STE and CMRI.

RV-oriented software using 3DE demonstrated good correlation with CMRI for RV volume measurements in HLHS patients.[8] Essentially, the 3D method does not use assumptions for computing ventricular volume, unlike volume calculation of the LV derived from 2D echocardiography. Hence, there may not be a significant difference in the volume evaluation between each 3D method. However, the border detection algorithm of RV-oriented software is based on a morphologically normal RV and the analysis is performed more automatically using machine learning in the current RV software, compared with older versions. As the result, it is possible that the automated algorithm may work poorly when the RV shape is complex or if the RV assumes a very different geometry after conversion to a functionally single RV (SRV).[16] In fact, we attempted to analyze RV volume and function of HLHS using RV-oriented software, but the tracking of the endocardial border was poor throughout the cardiac cycle.

RV Strain Analysis in HLHS

Both GCS and GLS obtained from 3D-STE correlated well with those from 2D-STE, although the magnitude of 3D-GCS was significantly higher than that of 2D-GCS.

Table 3. Segmental Strain Analyses in 3D-STE

Variable	Base	Mid	Apex	P value
PS (%)	−27.9±4.4	−29.3±5.2	−28.1±6.0	NS
CS (%)	−20.9±4.4*	−24.6±5.1	−24.1±6.0	<0.01
LS (%)	−18.1±3.4†	−17.4±3.4‡	−19.9±4.7	<0.01

Data expressed as mean±SD. Segmental strains were assessed by one-way ANOVA with post hoc analysis. *P<0.01 vs. Mid and Apex in CS, †P<0.05 vs. Apex in LS, ‡P<0.01 vs. Apex in LS. CS, circumferential strain; LS, longitudinal strain; PS, principal strain.

Previous studies demonstrated good agreement of conventional strains with CMRI in both functionally single LV (SLV) and SRV after Fontan palliation.[17,18] Moreover, Satriano et al showed good correlation of not only CS and LS but also PS between 3D-STE and CMRI in the LV.[14] However, because PS is a very new concept, so far there have not been any studies demonstrating correlation of PS and CMRI in children.

Our study showed a significant difference between 3D-GCS and 2D-GCS. Because a myocardial segment is a 3D structure, measuring the deformation of a 3D structure using a 2D modality such as 2D-STE can be hindered by the entrance and exit of speckles in the third dimension. This phenomenon may underestimate GCS measured in 2D-STE, because the fixed transversal slice crosses the ventricle at a level that becomes more basal (thus wider) while the base moves towards the apex during the contraction. 3D-STE may overcome this limitation of out-of-plane speckle loss noted in 2D-STE. Moreover, we performed segmental 3D strain analyses in the basal, mid, and apical segments to investigate the cause of differences between 3D-GCS and 2D-GCS. **Table 3** shows that 3D-CS at the base was significantly less than that in the mid- and apical-segments, which was not shown in the SLV.[17] We used basal CS as a value of 2D-GCS, similar to previous studies in which CS was smaller than LS.[10,11] However, 2D-GCS may be insufficient to represent global RV function of HLHS, which has a more complex shape than the LV and there is a drag on the deformation of the basal RV segment because of the presence of a rudimentary LV in HLHS.

Contribution of Strains to RV Function in HLHS

Our study revealed that peak GPS had the highest magnitude of strain among all strains and an extremely strong correlation with EF in HLHS patients after Fontan completion.

In contrast to CS and LS, the value of PS provides a main contractile force of deformation that is intrinsic to the tissue and not influenced by axis-dependent directions (**Figure 1**). Because of its 3D nature, it overcomes the problem of out-of-plane speckle loss; therefore, PS analysis can assess ventricular function without underestimation, which is particularly useful in the functionally SRV where the definition of anatomical direction, longitudinal and circumferential, can be less representative after transformation of the RV and the consequent alteration of myocardial fibers. The significance of PS has a firm theoretical background because it is based on all information present in the strain tensor and is not influenced by predefined assumptions. For this reason, too, it is the most common strain (or stress) property that is used in engineering applications involving multidirectional deformation.[19]

The analysis of PS also provides information about the orientation of deformation that is not necessarily aligned with the myofibers. Indeed, it is not an anatomical orientation and rather represents the dominant direction of contraction resulting from the contribution of myofibers along the thickness, counterwound between the endocardium and epicardium.[19,20] In-depth analysis of PS can describe not only the magnitude of the PS, but also the angle of the PS lines, reflecting the underlying myocardial architecture and function, by additional calculation using the coordinate data from 3D-STE.[19,20] A more recent study demonstrated the PS angle of the RV in the patients with pulmonary arterial hypertension changed from a more longitudinal to a more circumferential orientation, with increasing severity of pulmonary hypertension.[21] Such studies suggest that PS analysis would be more helpful for understanding the mechanics of RV function, including the direction of major myocardial deformation, which is not provided by conventional axis-dependent strains, such as LS and CS. Although in our study the angle of the PS lines was not assessed by the commercially available software, we speculate that newer calculations based on the entire information contained in the strain tensor will be available in the near future and may provide unique insights into the RV function of HLHS.

A previous study demonstrated the usefulness of area strain (AS) for assessing RV function.[22] AS represents the product of LS and CS and does not incorporate shear strains. In contrast, PS is based on an engineering model of a tensor, where shear strains are zero in the orientation of the principal strains and can be ignored. Therefore, PS has a somewhat stronger physics background that represents 3D strain more accurately. Moreover, compared with AS, PS lines can reflect the changes in myocardial architecture, leading to novel understanding of the mechanics of RV function.

In our comparison of GCS and GLS from 3D-STE, peak GCS had the higher magnitude of strain and stronger correlation with EF than peak GLS, which indicates the circumferential force was superior to longitudinal force for the RV function of HLHS. This contractile pattern resembles that seen in the morphologic LV[23] and has also been described in previous studies of functionally SRV and systemic RV after the atrial switch operation.[10,24] We speculate that this is an important compensatory mechanism in HLHS, which tends to have diminished LS.

Clinical Implications

In this preliminary study, we highlight the ability of 3D-STE to evaluate RV volumes and entire RV strains simultaneously, because it prove to be a promising index in HLHS, which lacks objective indices in the present era and is clinically assessed by qualitative methods.

Volume measurement is an essential parameter in the

management of patients with SV physiology, because dilatation of functionally SRVs may affect clinical outcomes.[1–3] The advantages of 3D-STE over CMRI are that it can be performed at the patient's bed-side without sedation and repeated assessments can be performed during outpatient visits. It is especially helpful in patients with implanted pacemakers or stents.[25] In addition, Ghelani et al indicate that not only ventricular dilation but also a decreasing GCS are associated with worse outcome.[26] Therefore, 3D-STE, which can assess ventricular volume and strain simultaneously, may be a valuable tool for predicting the outcome of HLHS patients.

Study Limitations

The first is lack of comparison with CMRI, which is often used as the gold standard. For the validation of 3D-STE in a HLHS cohort, a comparative study between 3D-STE and CMRI would be necessary. However, this study did indicate the usefulness of 3D-STE for assessing the RV function of HLHS by comparing 3DE and 2D-STE for the first time.

The second limitation is that PS is a brand-new concept even in the field of adult cardiology and has never been applied in pediatric cardiology. Therefore, a feasibility study needed to be performed. After establishing its feasibility, as with any new technique there is a learning curve involved, which needs to be overcome by repeated use. This is often the case whenever a new modality is introduced in echocardiography. Therefore, this new concept will to overcome the reticence on the part of physicians to become more accepted.

The median age of our study cohort was 10.6 years, at which obtaining 3D images by transthoracic echocardiography is easier than with adults. Therefore, it may be difficult to obtain sufficient 3D images for analyzing 3D-STE with increasing patient's age (e.g., in young adults with Fontan procedures). In addition, the relatively low frame rate of the 3D images in our study might also affect the measurements, typically resulting in underestimation of both strain and EF.

Conclusions

Our study showed the potential of utilizing the 3D-STE technique for simultaneous assessment of RV volume calculation and tissue deformation in HLHS. Analysis of a single 3D-STE clip of the cardiac cycle provides useful information regarding both volume and the functional status of HLHS, which can be useful during longitudinal follow-up as outpatients. In addition, PS is a promising, physics-based parameter to evaluate RV function in HLHS. These results may lead to further studies of the functional changes not only in HLHS, but other types of univentricular hearts as well.

Acknowledgments

We received partial support from the Italian Ministry of Education and Research, project PRIN no. 2017A889FP.

Disclosures

B.K. is a paid employee of TomTec Corporation, the maker of the software used in this project. Otherwise, we all have no disclosures of COI, grants, or funding related to the manuscript.

References

1. Martin BJ, Mah K, Eckersley L, Harder J, Pockett C, Schantz D, et al. Hypoplastic left heart syndrome is not a predictor of worse intermediate mortality post Fontan. *Ann Thorac Surg* 2017; **104:** 2037–2044.
2. Atz AM, Zak V, Mahony L, Uzark K, D'agincourt N, Goldberg DJ, et al. Longitudinal outcomes of patients with single ventricle after the Fontan procedure. *J Am Coll Cardiol* 2017; **69:** 2735–2744.
3. Piran S, Veldtman G, Siu S, Webb GD, Liu PP. Heart failure and ventricular dysfunction in patients with single or systemic right ventricles. *Circulation* 2002; **105:** 1189–1194.
4. Margossian R, Schwartz ML, Prakash A, Wruck L, Colan SD, Atz AM, et al. Comparison of echocardiographic and cardiac magnetic resonance imaging measurements of functional single ventricular volumes, mass, and ejection fraction (from the Pediatric Heart Network Fontan Cross-Sectional Study). *Am J Cardiol* 2009; **104:** 419–428.
5. Kutty S, Rathod RH, Danford DA, Celermajer DS. Role of imaging in the evaluation of single ventricle with the Fontan palliation. *Heart* 2016; **102:** 174–183.
6. Soriano BD, Hoch M, Ithuralde A, Geva T, Powell AJ, Kussman BD, et al. Matrix-array 3-dimensional echocardiographic assessment of volumes, mass, and ejection fraction in young pediatric patients with a functional single ventricle: A comparison study with cardiac magnetic resonance. *Circulation* 2008; **117:** 1842–1848.
7. Marx GR, Shirali G, Levine JC, Guey LT, Cnota JF, Baffa JM, et al. Multicenter study comparing shunt type in the Norwood procedure for single-ventricle lesions: Three-dimensional echocardiographic analysis. *Circ Cardiovasc Imaging* 2013; **6:** 934–942.
8. Bell A, Rawlins D, Bellsham-Revell H, Miller O, Razavi R, Simpson J. Assessment of right ventricular volumes in hypoplastic left heart syndrome by real-time three-dimensional echocardiography: Comparison with cardiac magnetic resonance imaging. *Eur Heart J Cardiovasc Imaging* 2014; **15:** 257–266.
9. Kutty S, Graney BA, Khoo NS, Li L, Polak A, Gribben P, et al. Serial assessment of right ventricular volume and function in surgically palliated hypoplastic left heart syndrome using real-time transthoracic three-dimensional echocardiography. *J Am Soc Echocardiogr* 2012; **25:** 682–689.
10. Tham EB, Smallhorn JF, Kaneko S, Valiani S, Mycrs KA, Colen TM, et al. Insights into the evolution of myocardial dysfunction in the functionally single right ventricle between staged palliations using speckle-tracking echocardiography. *J Am Soc Echocardiogr* 2014; **27:** 314–322.
11. Suntratonpipat S, Khoo NS, Colen T, Alhabdan M, Troung D, Zahari N, et al. Impaired single right ventricular function compared to single left ventricles during the early stages of palliation: A longitudinal study. *J Am Soc Echocardiogr* 2017; **30:** 468–477.
12. Flu WJ, van Kuijk JP, Bax JJ, Gorcsan J 3rd, Poldermans D. Three-dimensional speckle tracking echocardiography: A novel approach in the assessment of left ventricular volume and function? *Eur Heart J* 2009; **30:** 2304–2307.
13. Mangual JO, De Luca A, Toncelli L, Domenichini F, Galanti G, Pedrizzetti G. Three-dimensional reconstruction of the functional strain-line pattern in the left ventricle from 3-dimensional echocardiography. *Circ Cardiovas Imaging* 2012; **5:** 808–809.
14. Satriano A, Heydari B, Narous M, Exner DV, Mikami Y, Attwood MM, et al. Clinical feasibility and validation of 3D principal strain analysis from cine MRI: Comparison to 2D strain by MRI and 3D speckle tracking echocardiography. *Int J Cardiovasc Imaging* 2017; **33:** 1979–1992.
15. Kleijn SA, Brouwer WP, Aly MF, Rüssel IK, de Roest GJ, Beek AM, et al. Comparison between three-dimensional speckle-tracking echocardiography and cardiac magnetic resonance imaging for quantification of left ventricular volumes and function. *Eur Heart J Cardiovasc Imaging* 2012; **13:** 834–839.
16. Muraru D, Spadotto V, Cecchetto A, Romeo G, Aruta P, Ermacora D, et al. New speckle-tracking algorithm for right ventricular volume analysis from three-dimensional echocardiographic data sets: Validation with cardiac magnetic resonance and comparison with the previous analysis tool. *Eur Heart J Cardiovasc Imaging* 2016; **17:** 1279–1289.
17. Singh GK, Cupps B, Pasque M, Woodard PK, Holland MR, Ludomirsky A. Accuracy and reproducibility of strain by speckle tracking in pediatric subjects with normal heart and single

ventricular physiology: A two-dimensional speckle-tracking echocardiography and magnetic resonance imaging correlative study. *J Am Soc Echocardiogr* 2010; **11:** 1143–1152.
18. Salehi Ravesh M, Rickers C, Bannert FJ, Hautemann D, Al Bulushi A, Gabbert DD, et al. Longitudinal deformation of the right ventricle in hypoplastic left heart syndrome: A comparative study of 2D-featuretracking magnetic resonance imaging and 2D-speckle tracking echocardiography. *Pediatr Cardiol* 2018; **39:** 1265–1275.
19. Pedrizzetti G, Kraigher-Krainer E, De Luca A, Caracciolo G, Mangual JO, Shah A, et al. Functional strain-line pattern in the human left ventricle. *Phys Rev Lett* 2012; **109:** 048103.
20. Pedrizzetti G, Sengupta S, Caracciolo G, Park CS, Amaki M, Goliasch G, et al. Three-dimensional principal strain analysis for characterizing subclinical changes in left ventricular function. *J Am Soc Echocardiogr* 2014; **27:** 1041–1050.
21. Satriano A, Pournazari P, Hirani N, Helmersen D, Thakrar M, Weatherald J, et al. Characterization of right ventricular deformation in pulmonary arterial hypertension using three-dimensional principal strain analysis. *J Am Soc Echocardiogr* 2019; **32:** 385–393.
22. Ishizu T, Seo Y, Atsumi A, Tanaka YO, Yamamoto M, Machino-Ohtsuka T, et al. Global and regional right ventricular function assessed by novel three-dimensional speckle-tracking echocardiography. *J Am Soc Echocardiogr* 2017; **30:** 1203–1213.
23. Pedrizzetti G, Lapinskas T, Tonti G, Stoiber L, Zaliunas R, Gebker R, et al. The Relationship between EF and strain permits a more accurate assessment of LV systolic function. *JACC Cardiovasc Imaging* 2019; **12:** 1893–1895.
24. Pettersen E, Helle-Valle T, Edvardsen T, Lindberg H, Smith HJ, Smevik B, et al. Contraction pattern of the systemic right ventricle shift from longitudinal to circumferential shortening and absent global ventricular torsion. *J Am Coll Cardiol* 2007; **49:** 2450–2456.
25. Garg R, Powell AJ, Sena L, Marshall AC, Geva T. Effects of metallic implants on magnetic resonance imaging evaluation of Fontan palliation. *Am J Cardiol* 2005; **95:** 688–691.
26. Ghelani SJ, Colan SD, Azcue N, Keenan EM, Harrild DM, Powell AJ, et al. Impact of ventricular morphology on fiber stress and strain in Fontan patients. *Circ Cardiovasc Imaging* 2018; **11:** e006738.

Supplementary Files

Supplementary Movie 1. Analysis of 3D-STE in HLHS.

Supplementary Movie 2. Analysis of 3DE in HLHS.

Please find supplementary file(s);
http://dx.doi.org/10.1253/circj.CJ-19-0926